Photoconductivities of poly(N-vinyl carbazoles) containing cation radicals

H. Block, Sheelagh M. Bowker and S. M. Walker
Department of Inorganic, Physical and Industrial Chemistry, Donnan Laboratories, University of Liverpool, PO Box 147, Liverpool L69 3BX, UK
(Received 13 November 1977)

A study into the photoconductance of poly(N-vinyl carbazole) partly oxidized to introduce cation radicals is described (mole fraction $< 4 \times 10^{-3}$). These materials are shown to be photoconductors whose response to illumination is time dependent. Their photoconductive behaviour has been studied as a function of extent of oxidation, field strength, temperature, light intensity and irradiating wavelength. The observed response is discussed in terms of a model for the amorphous state in which there are accessible levels in the forbidden gap for interaction with photopromoted electrons or holes. Variation in the role of level as trap or recombination centre with external conditions is shown to form, in part, an adequate model for behaviour. However, light intensity and temperature dependence does indicate that there is a significant change of the distribution of levels in the forbidden gap as the temperature is reduced to $\sim -20°C$, possibly due to a change in structure or mode of motion.

INTRODUCTION

It has been known since 1957 that poly(N-vinyl carbazole) (PNVC) is a photoconducting polymer[1] with its major response to radiation occurring at wavelengths (λ) of about 400 nm and below. The majority carriers in the photoconductivity of PNVC appear to be holes, and the process has a low activation energy variously reported as between 0.12 and 0.65 eV[2-5]. Authors either have described the process as involving a hopping mechanism[2,6] or alternatively band transport with strong trapping[2]. A study of a highly crystalline sample of PNVC suggested that migration along the chain from carbazole unit to carbazole unit was taking place[5,8]. Workers[5,8] found that the nature of the electrode is significant in PNVC photoconductance and when present, such participation is consistent with a process of hole injection at the electrode—polymer interface. This has been reported[9] to occur even in the visible region of the spectrum when high field strengths (E) are used.

PNVC can be sensitized to respond more actively in the visible region of the spectrum. This is generally achieved either by incorporating dyestuffs as optical sensitizers or by making use of the propensity of the carbazole unit for forming coloured charge transfer complexes with acceptor molecules to provide chemical sensitization. 2,4,7-Trinitrofluorenone (TNF) has found particular favour as a chemical sensitizer for applications in electroimaging devices[10]. Optical or chemical sensitization involves the introduction of extra absorption bands into the visible, some of which are responsible for the photoactivity. It is a noticeable feature of many such enhanced systems that the photoconductive response is much broader as a function of wavelength than absorption, and sensitized PNVC systems are often panchromatic. Aspects of the physics of the PNVC/TNF system differ from undoped PNVC. In particular, both hole and electron migration appear to take part, the electron mobility being associated with the carbazole—TNF complex whilst hole mobi-

lity is retained for uncomplexed carbazole residues[4]. Both alternative mechanisms of transport by hopping[4] or by trap-controlled band conductance[11] have been invoked for the PNVC/TNF system.

We have reported recently that the chemical introduction of cation radicals into PNVC considerably enhances its semi-conductivity[12]. The required oxidation is readily performed using tris(p-bromophenyl)ammoniumyl salts on PNVC as substrate, and involves a 3 electron abstraction with carbazole ring dimerization via the 4-position[13]. The extent of reaction and hence the radical concentration (mole fraction, x) are controllable stoichiometrically. Here we report that at low x such PNVC/cation radical systems also exhibit significant photoconductivity. Illumination of oxidized PNVC with visible radiation causes the development of a photocurrent. We have studied the magnitude and rate of establishment of such photocurrents as a function of x, λ, light intensity, I, and temperature, T. The behaviour, which shows considerable diversity in its dependence on these variables, can be rationalized largely in terms of the band theory with traps and recombination centres developed principally by Rose[14] and applied to PNVC photoconductance by Pai[15].

EXPERIMENTAL

Materials

Cation radical-containing PNVC was prepared from a commercial sample of PNVC (weight-average molecular weight 1.25×10^6) by oxidation with tris(p-bromophenyl) ammoniumyl hexachloroantimonate(V) using dichloromethane as solvent. Details of the reaction conditions have been reported previously[12]. Samples were prepared to low degrees of oxidation ($x < 4 \times 10^{-3}$, for individual values see *Table 1*). Higher concentrations of cation radicals pro-

Table 1 Characteristic data for cation radical-containing PNVC samples

| | Sample code | | | | |
	PNVC	1	2	3	4
$10^4 x$	0	0.2	0.8	23.7	39.0
$\sigma_{293}(ohm^{-1} cm^{-1})$*	4.2×10^{-16}	2.6×10^{-15}	2.1×10^{-14}	3.7×10^{-13}	10^{-11}
Film thickness (μm)	20	35	27	23	30
i_D (amp)†	4.2×10^{-11}	3.3×10^{-11}	2.5×10^{-10}	5.2×10^{-8}	1.3×10^{-7}
i_P^∞ (amp)	$<5 \times 10^{-12}$	5.5×10^{-9}	7.3×10^{-9}	5.6×10^{-8}	2.4×10^{-8}
Activation energies (eV)					
Dark >270K	—	—	0.42	0.46	—
Dark <270K	—	—	0.11	0.29	—
Photo- >260K	—	—	0.31	0.43	—
Photo- <260K	—	—	0.31	0.23	—

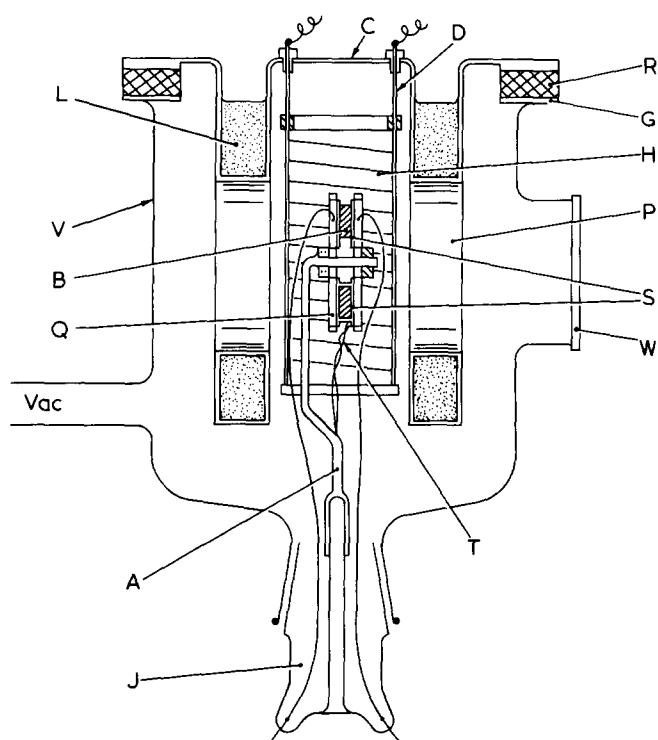* Specific conductivity in the dark at 293K; † measured in the ohmic region at 20 V and 293K

Figure 1 Cell for measuring semi- and photoconductance as a function of temperature

duced materials in which any photoconductance was swamped by their substantial semiconductance.

In order to obtain films suitable for photoconductance experiments, solutions of the oxidized polymers in dichloromethane (2% w/v) were allowed to evaporate from mercury surfaces for 48 h. This technique produced somewhat brittle films, which after removal from the mercury were vacuum dried for a further 48 h. Regions with suitable uniformity of film thickness were achieved by utilizing a mercury surface area much larger than that required for the sample. Thus, since disc electrodes of 15 mm diameter were used on the film, circular mercury surfaces $\geqslant$ 5 cm were used for casting. Both film uniformity and mean thickness were measured with a micrometer: variation in thickness for the selected regions was <15%. After casting and selection of a suitable site (usually in the central part), a square piece of film was cut from that region, having sides slightly larger than 15 mm. Subsequently, and with the aid of a PTFE

mask, 15 mm circular gold/palladium electrodes were evaporated onto the film. This was done using an Edwards model 6E4 coating unit operated under standard conditions to ensure reproducibility in the film transmittance. These conditions involved using a standard length of gold/palladium (40/60) wire on the tungsten filament whose spatial position together with that of the film with mask were kept identical for all evaporations. Complete evaporation of the gold/palladium sample was carried out at a pressure of 1.5 x 10^{-4} torr. Photometric transmittance tests showed that this standard procedure ensured a reproducibility of 5%.

Measurements

Photo- and semiconductivities of the polymer films were measured by the use of the equipment shown in *Figure 1*. The samples S plus 15 mm diameter brass spacers B are mounted between quartz plates Q carrying semitransparent electrodes. These were of gold/palladium, prepared by evaporation and of measured transmittance. Each plate carried an upper and lower electrode; however, only the former acted as a contact system and to this end was connected at the edge of the quartz plates to leads by means of silver-filled epoxy adhesive. The duplicate lower dummy electrode system, brass spacer and sample carried a chromel/alumel thermocouple T. The whole of the quartz plate—sample assembly system was mounted via a central fixing hole, brass rod and spring system A to the joint J which also carried the sealed thermocouple and current leads. By use of the joint J, the experimental sample could easily and accurately be located centrally in the thermostatically controlled system. This consisted of an open (2 mm spacing) box-like nichrome wire wound heater H of 30 Ω resistance which in turn was surrounded by the stainless steel cooling jacket, C. The window W, porthole P and open mesh of heater H enable both experimental and dummy samples to be irradiated. For temperatures below ambient, a coolant L such as liquid N_2 was introduced into the jacket C. Problems of thermal contraction of C were overcome by incorporating a silicone rubber pad R between the rim of C and a glass annulus G, contact surfaces between C, R and G being bonded with silicone rubber. This assembly then provides a conventional glass flange joint between vessel V and C which can withstand the thermal shock. The heater wiring was supported on an open framework brass cage with glass sleeve insulation (not shown), of which two corner rods, D, acted as electrical contacts. These were located via PTFE insulators into the upper surface of jacket C.
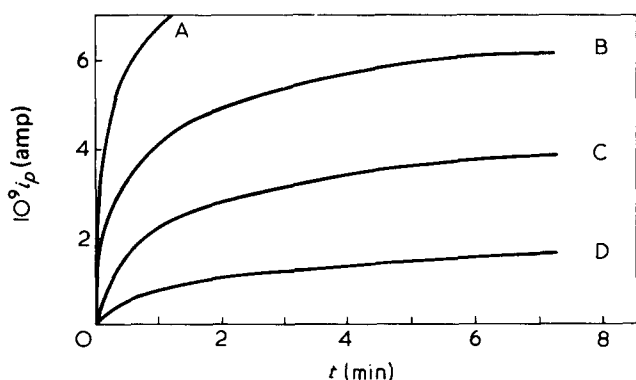
Figure 2 The photoresponse of sample 3 at 20°C under illumination. Light intensities (lux) A, 87; B, 41; C, 20 and D, 6

Thermal control of the samples to ±2°C can be achieved by a combination of constant current through H and, for experiments below ambient, cooling via C plus evacuation of the vessel V (≤10^{-2} torr). Because of the small heat capacity of the sample/electrode system a wide temperature range is accessible (−100° to +200°C), although in the present study the temperature was not increased above 60°C to avoid sample deterioration. A control experiment with thermocouples sited under both films (no voltage applied) showed that the upper and lower samples were maintained at identical temperatures.

For conductance measurements the measuring sample electrodes were connected in series with a Wareham S07 constant voltage source and Keithley Model 602 electrometer acting as ammeter whose output was recorded as a function of time. Connections were made using screened (earthed) coaxial leads and the vessel V and electrometer were placed inside an earthed aluminium box. This ensured both the exclusion of light and reduction of electrical noise. A shutter in the box enabled the sample to be exposed to exterior illumination.

The light source consisted of a collimated beam of light obtained with lenses and an iris diaphragm, and originating from a 250 W medium pressure mercury lamp. Thermal radiation was removed by a water tank, a selective (gelatin) or continuously adjustable interference (Veril S200) filter was used to select and vary λ, and neutral density filters were incorporated to alter the light intensity. The illumination intensities incident at the outer surface of Q were determined using a calibrated Mullard RPY 71 CdS photocell which was inserted instead of the electrode system for this measurement. No experiments were performed until a ½ h period had elapsed for lamp warm-up, and the intensity at Q was checked periodically to detect lamp ageing. Transmittances of Q, the evaporated electrodes and the samples were measured using an SP8000 u.v. spectrophotometer.

RESULTS AND DISCUSSION

All the samples containing cation radicals with $x \leqslant 4 \times 10^{-3}$ exhibited measurable photoconductive effects upon illumination with visible radiation. This contrasts with the lack of response observed in PNVC. The magnitude of the photocurrent, i_p, defined as the enhanced current above dark current, i_D, did not, as was the case with i_D, increase dramatically with x (*Table 1*). For sample 1 a long period of illumi-

nation with 540 nm radiation of 85 lux intensity resulted in an increase > 150 times i_D whilst sample 4 under the same conditions provided an increase of only ~0.2 in current level. Whether oxidized PNVC of $x > 4 \times 10^{-3}$ would show any photoconductance remains an open question since, were it to contribute at the same level as in samples 1−4, discriminations of such small currents additional to i_D are not possible with the present equipment.

As has already been indicated, we observed a time lag in the development of the photoresponse. Even the dark current component required a period to reach a steady value, the requirement being longer for samples of low x. It is our view that the time dependence, t, for the dark current is a capacitative effect since the response took the form of an overshoot in current (charging current) followed by an exponential decay to the steady state value. For photocurrent measurements, the steady state dark current was established before illumination. The photoresponse was then recorded as a function of time, examples being shown in *Figure 2*. Such a lag in response for photoconductors is a well known phenomenon[14] and presents some problems in quantifying the influence of variables such as T, E, λ, I and x. We have characterized curves such as those shown in *Figure 2* firstly by establishing values of i_p^∞ as $t \to \infty$. This has been possible since for all curves at sufficiently large t, the following equation was found to apply:

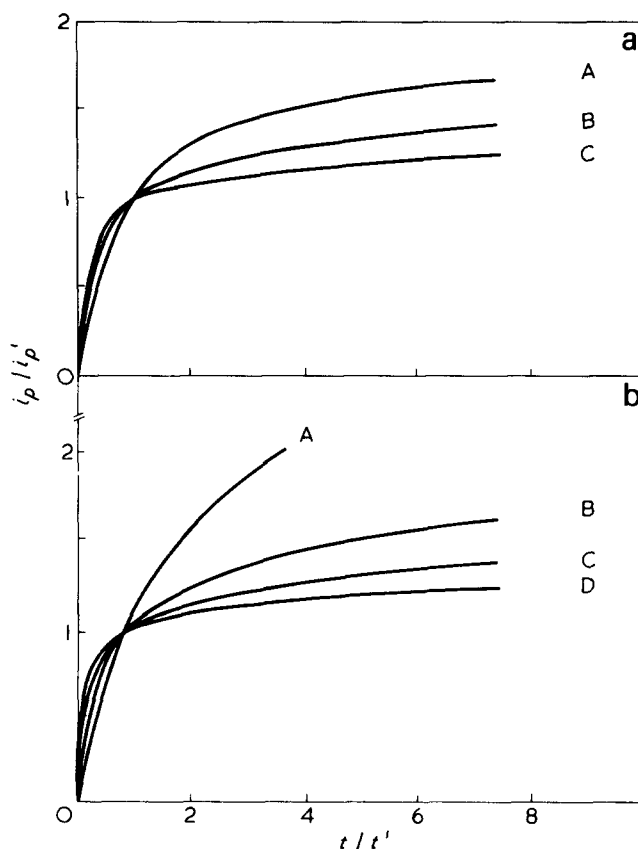*Figure 3* Reduced variable plots of photoresponse under differing intensities of illumination (I) and constant temperature (20°C). (a) Sample 2: A, I = 7.5 lux, i_p^∞ = 2.2 × 10^{-10} amp, t' = 52 sec; B, I = 15 lux, i_p^∞ = 6.0 × 10^{-10} amp, t' = 80 sec; C, I = 87 lux, i_p' = 3.1 × 10^{-9} amp, t' = 22 sec. (b) Sample 3: A, I = 3 lux, i_p^∞ = 1.7 × 10^{-10} amp, t' = 5.3 sec; B, I = 24 lux, i_p^∞ = 3.6 × 10^{-9} amp, t' = 40 sec; C, I = 41 lux, i_p^∞ = 6.9 × 10^{-9} amp, t' = 55 sec; D, I = 87 lux, i_p' = 2.6 × 10^{-8} amp, t' = 18 sec
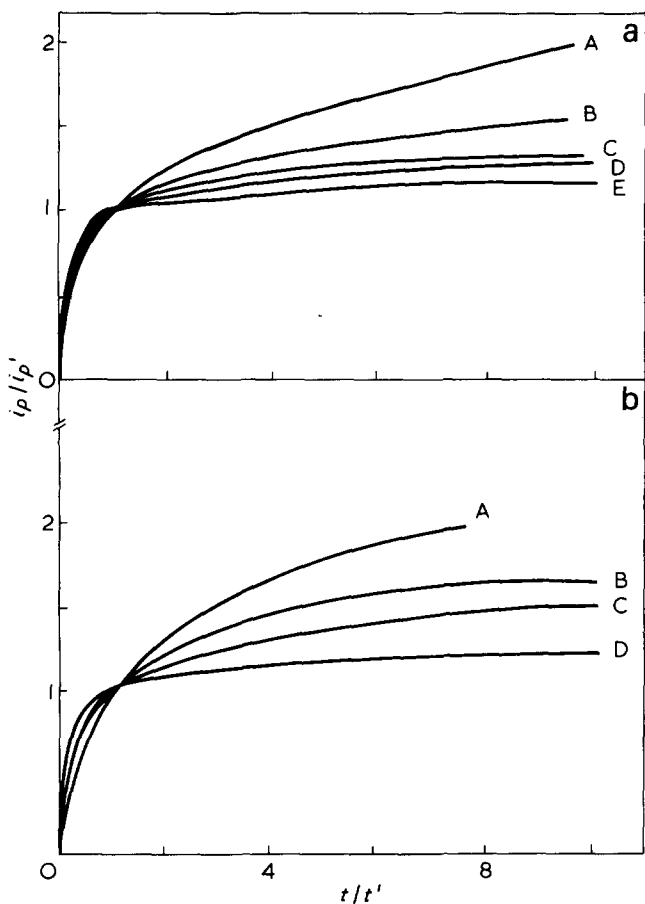
Figure 4 Reduced variable plots of photoresponse at differing temperatures (T) and constant illumination (87 lux). (a) Sample 2: A, $T = -39°C$, $i'_p = 2.9 \times 10^{-10}$ amp, $t' = 46$ sec; B, $T = -17°C$, $i'_p = 3.8 \times 10^{-10}$ amp, $t' = 53$ sec; C, $T = 25°C$, $i'_p = 3.0 \times 10^{-9}$ amp, $t' = 27$ sec; D, $T = 37°C$, $i'_p = 5.9 \times 10^{-9}$ amp, $t' = 36$ sec; E, $T = 60°C$, $i'_p = 7.4 \times 10^{-9}$ amp, $t' = 7.7$ sec. (b) Sample 3: A, $T = -53°C$, $i'_p = 5.3 \times 10^{-11}$ amp, $t' = 10$ sec; B, $T = -20°C$, $i'_p = 6.5 \times 10^{-10}$ amp, $t' = 15$ sec; C, $T = 2°C$, $i'_p = 2.2 \times 10^{-8}$ amp, $t' = 23$ sec; D, $T = 35°C$, $i'_p = 2.6 \times 10^{-8}$ amp, $t' = 18$ sec

$$i_p/i_p^\infty = 1 - \exp(-t/\tau) \tag{1}$$

Since equation (1) does not always hold at short times, because of either the intrinsic theoretical grounds or response problems due to instrumental inertia, equation (1) does not characterize all response behaviour at all times. Secondly, in order to compare curves which from experiment to experiment sometimes involve vastly different magnitudes, results were scaled to i_p and t' values at which $di_p/dt = 1$, using a computer analysis of data input. The program replotted data in the reduced variables i_p/i_p and t/t'. The influence of I or T on photoresponse becomes more readily compared in such reduced variables as shown in *Figures 3* and *4*. At sufficiently low field strengths all the samples studied behaved ohmically but both dark and photocurrents became superlinear in E at values approaching 10^6 V/m. This onset of superlinearity in i_p^∞ also appeared to be light dependent (*Figure 5*). Temperature variation was characterized by Arrhenius plots of i_p^∞ and i_D (*Figure 6*) and it can be seen that the activation energies for photo- and semi-conductivities are similar (*Table 1*). In some cases, two processes of differing activation energy are observed. Such effects in these materials have not been reported previously because the investigation of semiconductivity[12] was instrumentally restricted to a narrower temperature range. Varia- ,

tion of i_p^∞ with I was studied for sample 3 (*Figure 7*). At temperatures near ambient, the photocurrent was first order in light intensity but at lower temperatures this dropped to 0.53. That wavelength response was essentially panchromatic in the experimental region (400–600 nm) is illustrated in *Figure 8*, which shows the close similarity in photoresponse and lamp emission power[16].

In their behaviour, these samples of partly oxidized PNVC show many well known aspects of photoconductance in amorphous materials and as such support the mechanistic ideas largely due to Rose[14]. Thus it appears that the inclusion of cation radicals into PNVC at low concentration introduces a large number of states which act as traps or re-
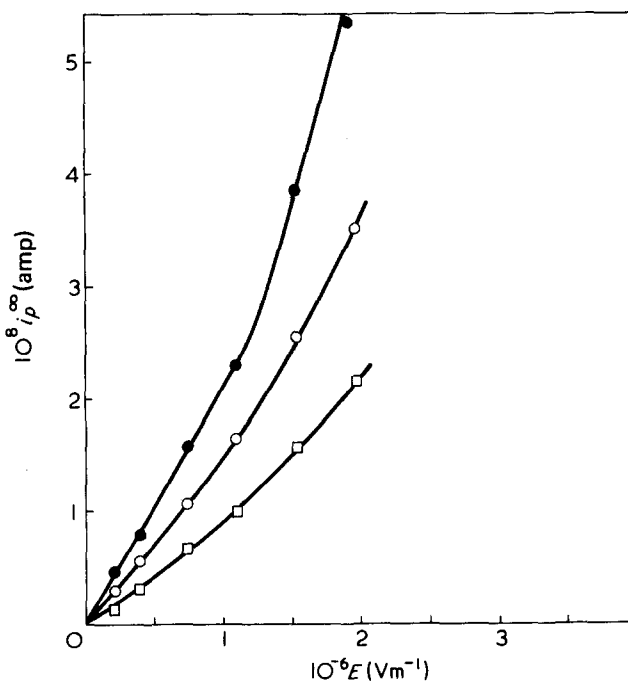

Figure 5 The variation of photocurrent with applied field (E) for sample 3 at 20°C. Light intensities: ●, 87 lux; ○, 41 lux; □, 20 lux
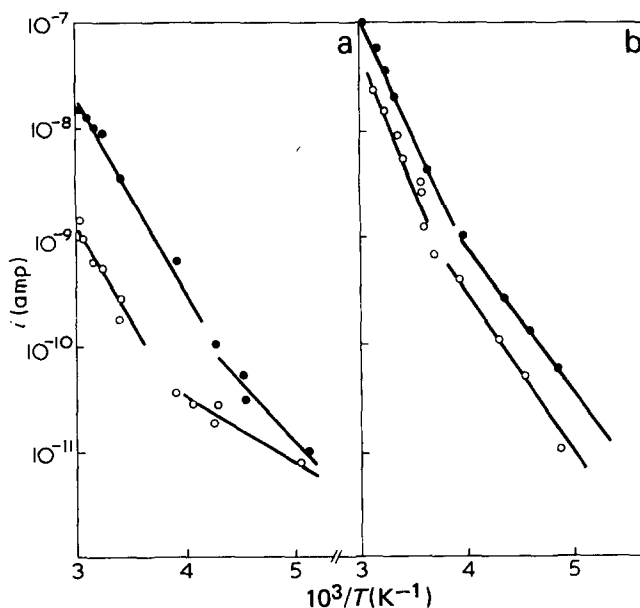

Figure 6 Arrhenius plots for dark current (○) and equilibrium photocurrent (●) at a constant illumination of 87 lux. (a) sample 2 and (b) sample 3
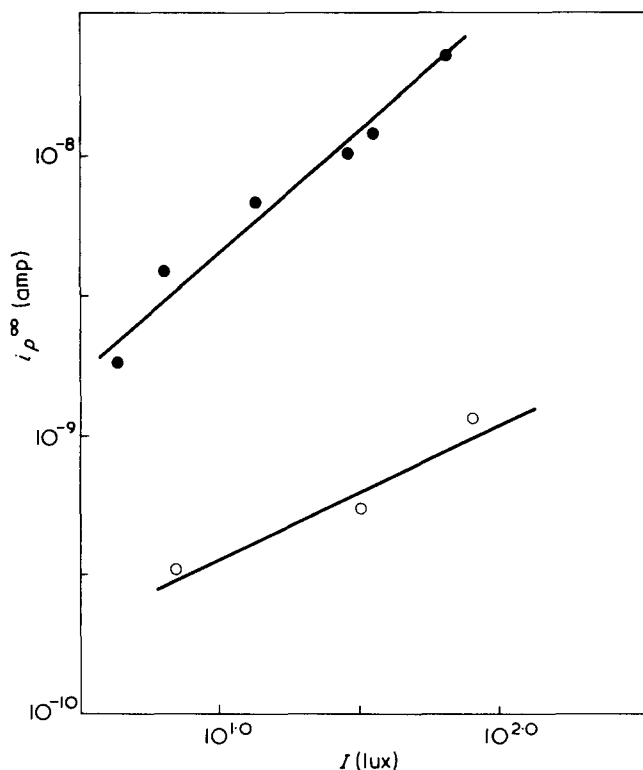
Figure 7 The dependence of equilibrium photocurrent (i_p^∞) on light intensity I for sample 3. Temperature: ●, $20°C$; ○, $-20°C$

Figure 8 The wavelength (λ) dependence of equilibrium photocurrent (a) and lamp emission power (b) for sample 3 at $20°C$

combination centres. At the low levels of light intensity attainable and at the higher temperatures, the hole and electron demarcation levels which energetically separate the role of trap state from recombination centre, are well removed from the conduction (electron migration) or valence (hole migration) bands. This leaves a large population of states acting as traps in the forbidden gap. Although the present investigation provides no evidence as to whether holes or electrons are the dominant or only carriers, the effect of accessible traps but relatively inaccessible recombination centres results in the first order creation or decay of carriers. In consequence we observe an approximately exponential dependence in response, which because of the large trap concentration shows a response time greatly in excess of the expected carrier lifetime. The fact that at moderate temperatures the attainable level of photocurrent is first order in I (*Figure 7*) leads to the deduction that there is a wide distribution (in energetic terms) of levels throughout the forbidden zone. However, at lower temperature this first order dependence is not maintained; the light intensity dependence becomes half order and changes quite sharply over a limited temperature range. According to the model of Rose, an exponent of 0.5 in I is characteristic of a cluster of levels acting as traps which are not readily converted to recombination centres by the light intensity available. Thus it appears that at these low temperatures the demarcation levels can never reach the lowest trap levels. At higher temperatures the demarcation levels do sweep through the levels in the forbidden gap since the exponent in I is 1.0. The narrow temperature range over which the change occurs and the fact that the exponent changes from 0.5 to 1.0 with increasing T suggests a change in the trap levels from shallow to both shallow and deep traps with increasing T. The sharpness of the change appears to indicate that this shift in levels may be consequent upon either a
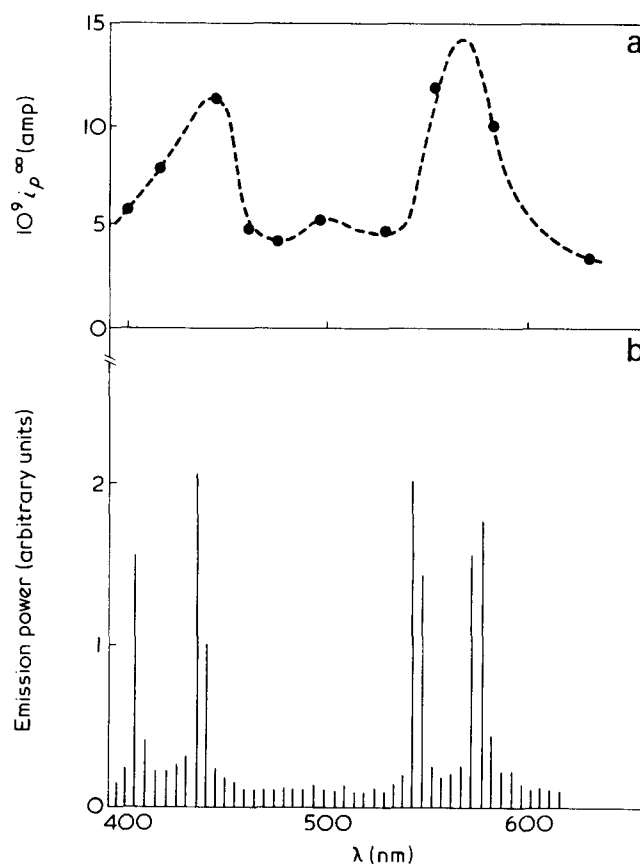
structural transition or the onset of a mode of motion. An independent observation consistent with this is the change in activation energy with temperature: at low temperatures, the photoconductance is energetically easier, consistent with shallow traps. These results are suggestive at a molecular level, indicating the possibility of coupling between cation radical sites and neighbouring carbazole residues. This could lead to radical delocalization with resonance energy thus generating shallow traps. Increasing temperatures will, by phonon scattering, tend to disrupt such coupling and produce a wider distribution of trap levels. The double linear nature of the Arrhenius plots (*Figure 6*) with its sharp transition, mirrors the light intensity dependence and supports the view that the onset of a structural change or mode of motion occurs in these systems.

ACKNOWLEDGEMENTS

REFERENCES

1   Hoegl, H., Sus, O. and Neugebauer, W. W. Ger. Pat. 1 068 115 (1957)
2   Szymanski, A. and Labes, M. M. *J. Chem. Phys.* 1969, **50**, 3568
3   Gill, W. D. *J. Appl. Phys.* 1972, **43**, 5033
4   Chen, I. and Slowik, J. M. *Solid State Commun.* 1975, **17**, 783

5 Lakatos, A. I. and Mort, J. *Phys. Rev. Lett.* 1968, **21**, 1444
6 Gibbons, D. J. and Spear, W. E. *J. Phys. Chem. Solids* 1966, **27**, 1917; Chen, I. *J. Chem. Phys.* to be published and quoted in ref (15)
7 Kimura, A., Yoshimoto, S., Akana, Y., Hirata, H., Kusabayashi, S., Mikawa, H. and Kasai, N. *J. Polym. Sci. (A-2)* 1970, **8**, 643
8 Reucroft, P. J. and Ghosh, S. K., *Phys. Rev. (B)* 1973, **8**, 803
9 Mort, J. and Lakatos, A. I. *J. Non-Cryst. Solids* 1970, **4**, 117
10 *Prod. Eng.* May 1970, p 50
11 Hoegl, H. *J. Phys. Chem.* 1965, **69**, 755; Seki, H. and Gill, W. D. *Int. Conf. on Conduction in Low Mobility Materials, Eilat, Israel,* 1971
12 Block, H., Cowd, M. A. and Walker, S. M. *Polymer* 1977, **18** 781

13 Iles, D. H. and Ledwith, A. *Chem. Commun.* 1968, p. 498; Beresford, P., Iles, D. H. Kricka, L. J. and Ledwith, A. *J. Chem. Soc. Perkin Trans.* 1974, p. 276
14 Rose A., *RCA Rev.* 1951, **12**, 362; 'Photoconductivity Conference', Wiley, New York, 1959, p. 3; *Proc. IRE* 1955, **43**, 1850; *Phys. Rev.* 1955, **97**, 322; *Prog. Semicond.* 1957, **2**, 109; 'Concepts in Photoconductivity and Allied Problems', Interscience Tracts on Physics and Astronomy, No. 19, (Ed. R. E. Massbak), Interscience, London, 1963
15 Pai, D. M. 'Introduction to Photoconductivity in Solids. Photoconductivity in Polymers: An Interdisciplinary Approach'. (Eds A. V. Patsis and D. A. Seanor), Technomic Publishing Co., Westport 1976, p. 28
16 Calvert, J. G. and Pitts, J. N. 'Photochemistry' Wiley, 1966, p.696